Charge Ordering and Sound Velocity Anomaly in La$_{1-X}$Sr$_X$MnO$_3$ ($X \geq 0.5$)

Hiroyuki Fujishiro, Tetsuo Fukase[1] and Manabu Ikebe

*Department of Materials Science and Technology, Faculty of Engineering, Iwate University,
4-3-5 Ueda, Morioka 020-8551*
[1] *Institute for Materials Research, Tohoku University, 2-1-1 Katahira, Aoba, Sendai 980-8577*

The electrical resistivity, magnetization, dilatation and sound velocity have been measured for La$_{1-X}$Sr$_X$MnO$_3$ ($0.48 \leq X \leq 0.90$) polycrystals. Observed anomalies in the sound velocity and the dilatation strongly suggest the occurrence of the charge ordering within the Sr-concentration range $0.48 \leq X \leq 0.82$. A phase diagram of the charge-ordered state in La$_{1-X}$Sr$_X$MnO$_3$ as a function of temperature T and the Sr concentration X is proposed.

As recent revived studies on perovskite-based manganites have confirmed, R$_{1-X}$A$_X$MnO$_3$-type crystals (R=La and trivalent rare earth ions, A=Sr, Ba, Ca)[1-5] undergo a variety of phase transitions which originate from the interplay and competition of various physical interactions. The most conspicuous transition may be the one from an antiferromagnetic (AFM) insulator to a ferromagnetic (FM) metal, leading to a colossal magnetoresistance (CMR) of these systems. The FM metallic state in the doped manganites is caused by the double exchange mechanism and the ferromagnetic alignment of Mn^{4+} ($S = 3/2$) spins is stabilized by fully polarized e_g-band electrons. However, as a result of competition with AFM superexchange or polaron ordering,[6-8] the FM metallic state is often unstable against the formation of charge ordering (CO) and a commensurate fraction of the carrier concentration such as $X = 1/8$, $1/3$, $1/2$ and $2/3$ is expected to favor a particular type of CO. The charge ordering near $X = 1/2$ has been reported for several systems such as Pr$_{1-X}$Ca$_X$MnO$_3$,[9-12] Pr$_{1/2}$Sr$_{1/2}$MnO$_3$,[13-15] Nd$_{1/2}$Sr$_{1/2}$MnO$_3$[15-17] and La$_{1-X}$Ca$_X$MnO$_3$.[3-5] The type of AFM order below the CO transition has been reported mostly to be of the CE-type[3] for $X \approx 1/2$ with some exceptions.[15] Very recently, Akimoto *et al.*[18] observed the A-type AFM structure for La$_{0.46}$Sr$_{0.54}$MnO$_3$ single crystals associated with the occurrence of CO.

In a previous study,[19] we reported CO in La$_{1-X}$Sr$_X$MnO$_3$ centered at $X = 1/8$ and pointed out that the sound velocity anomaly can be a very sensitive and useful measure to monitor the occurrence of CO in this system. For La$_{1-X}$Sr$_X$MnO$_3$ with a large e_g-electron bandwidth (W), the charge ordering at $X \approx 0.5$ was believed to be absent. However, we have found a clear sign of the occurrence of CO in La$_{1-X}$Sr$_X$MnO$_3$ polycrystals at $X \approx 0.5$ from the magnetization and resistivity measurements.[20] In this letter, we present the data of the sound velocity, thermal expansion, magnetization and electrical resistiv-

ity as a function of temperature, extending the range of X up to 0.90. The results suggest that CO occurs over a wide Sr concentration $0.48 \leq X \leq 0.82$ besides the one centered at $X = 1/8$.[8, 19, 20]

La$_{1-X}$Sr$_X$MnO$_3$ samples were prepared from stoichiometric mixtures of La$_2$O$_3$, SrCO$_3$ and Mn$_3$O$_4$ powders.[19] The mixtures were calcined twice at 1000°C for 24 h in air, pressed into pellets and then sintered at 1500°C for 8 h in air. The sintered crystals were heat-treated at 1500°C for 24 h in flowing oxygen. All the samples were confirmed to be in a single phase at room temperature using X-ray diffraction analyses. The measured densities of each sample were higher than 85% of that of the ideal one. The magnetization $M(T)$ was measured using a commercial SQUID magnetometer from 10 K to 400 K under an applied magnetic field of 5000 G. The sound velocity $v_s(T)$ was measured using the pulse-superposition method between 4.2 K and 290 K, by applying 7 MHz longitudinal sound waves.[19] The dilatation d$L(T)/L$ was measured between 90 K and 370 K using the strain-gauge method.

Figures 1(a) and 1(b) show the magnetization $M(T)$ of La$_{1-X}$Sr$_X$MnO$_3$ samples as a function of temperature T. For $X = 0.48$, the FM transition occurs at the Curie temperature $T_c = 330$ K and the FM state is stable over the entire temperature range below T_c. For $X = 0.50$, 0.52 and 0.55, however, the FM state becomes unstable at lower temperatures and the AFM order sets in as indicated by a sharp drop in $M(T)$ at T_N.[20] For $X \geq 0.60$, the FM state disappears completely and only the AFM order occurs as indicated by the cusps of the $M(T)$ curves. The behavior of $M(T)$ bears a close resemblance to that of La$_{1-X}$Ca$_X$MnO$_3$.[4]

Figures 2(a) and 2(b) show the temperature dependence of the electrical resistivity $\rho(T)$ of La$_{1-X}$Sr$_X$MnO$_3$ polycrystals for $X \geq 0.48$. The $\rho(T)$ curves for $X < 0.48$ are reported in our previous papers.[19, 20] The resistivity $\rho(T)$ of La$_{0.52}$Sr$_{0.48}$MnO$_3$ in
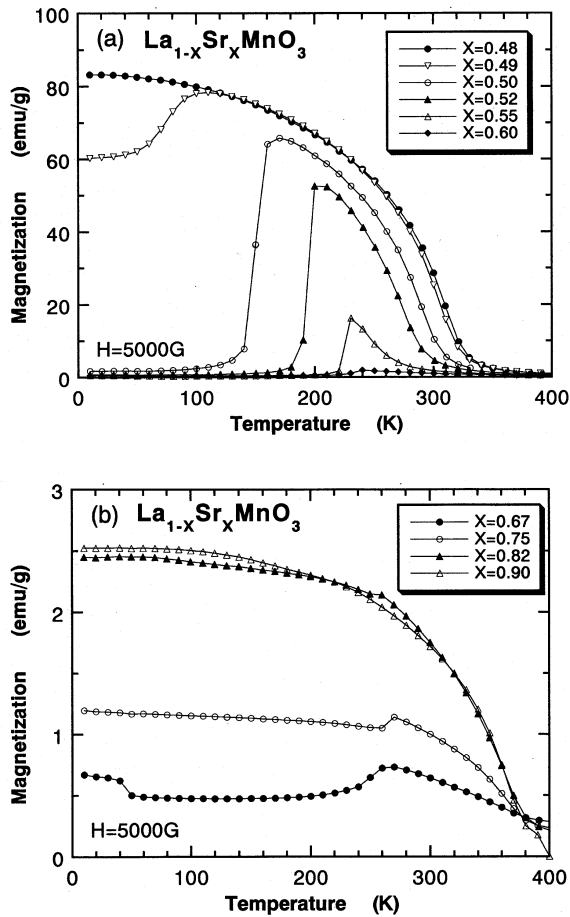
Fig. 1. The magnetization of $La_{1-X}Sr_XMnO_3$ samples under an applied field of 5000 G for (a) $0.48 \leq X \leq 0.60$ and (b) $0.67 \leq X \leq 0.90$.
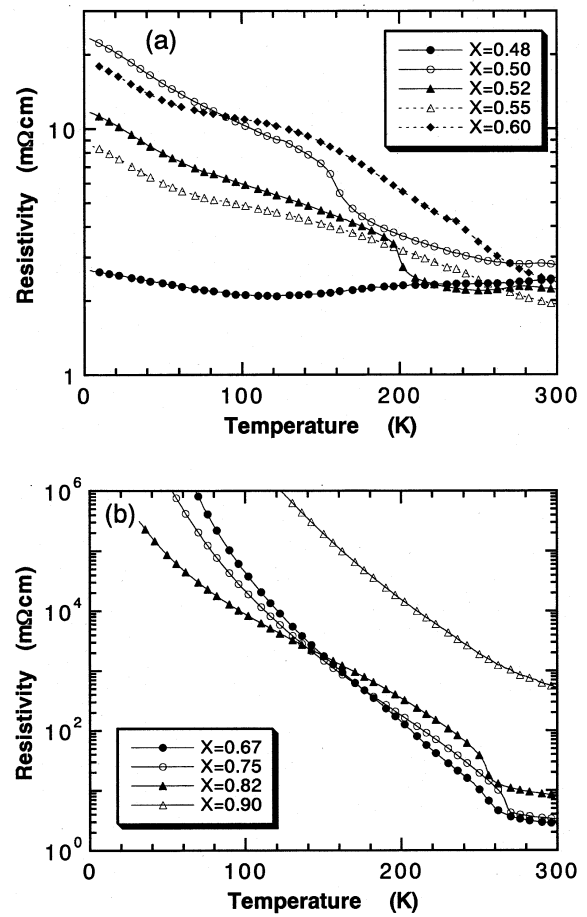

Fig. 2. The temperature dependence of the electrical resistivity $\rho(T)$ of $La_{1-X}Sr_XMnO_3$ samples for (a) $0.48 \leq X \leq 0.60$ and (b) $0.67 \leq X \leq 0.90$.

Fig. 2(a) attains a minimum at around 130 K and shows a semiconductive behavior below this temperature. The semiconductive behavior of $\rho(T)$ becomes more distinct with increasing Sr concentration X. For $X = 0.50$ and 0.52, abrupt increases in $\rho(T)$ are noticed at around 150 K and 200 K, which correspond to the onset of the AFM order observed in the $M(T)$ curves in Fig. 1(a). It is worthwhile to notice that the absolute values of $\rho(T)$ increase rather abruptly between $X = 0.60$ and $X = 0.67$ with increasing X. The present $La_{1-X}Sr_XMnO_3$ samples may be divided into two groups; the low-resistivity group for $0.48 \leq X \leq 0.60$ given in Fig. 2(a) and the high-resistivity group for $X \geq 0.67$ given in Fig. 2(b). Because $La_{1-X}Sr_XMnO_3$ polycrystals are not metallic for $X \geq 0.48$, at least at low temperatures, we classify all the samples in this work as insulators.

Figure 3 shows the sound velocity $v_s(T)$ as a function of T for typical samples. For $X = 0.50$, 0.52 and 0.55, the $v_s(T)$ curves show clear anomalies which explicitly correspond to those of the magnetization at the onset of the AFM order. However, the anomaly in $v_s(T)$ occurs not only in the vicinity of $X = 0.5$ but continuously persists into larger X regions where competition between the FM and AFM orders is not observable. The forms of the $v_s(T)$ anomalies are somewhat different for $X \leq 0.50$ and $X \geq 0.52$. For $X = 0.48$ and $X = 0.50$, the anomaly

appears as an abrupt increase of $v_s(T)$ with decreasing temperature (one should not overlook the anomalous increase in $v_s(T)$ at around 50 K for $X = 0.48$). In contrast, the anomaly appears as a local minimum in $v_s(T)$ for $X \geq 0.52$ accompanied by a considerable softening of the lattice. The magnitudes of the anomalies seem to be the largest for $X = 0.67$ or $X = 0.75$.

The temperature dependence of the dilatation dL/L between 100 K and 290 K is shown in Fig. 4. Except for $X = 0.48$, dL/L shows anomalies at exactly the same temperatures where $v_s(T)$ shows significant anomalies. What is to be noticed in this figure is that the anomalies show quite an opposite character for $X \leq 0.60$ and $X \geq 0.67$; with decreasing temperature, dL/L abruptly decreases at the anomaly for $X \leq 0.60$, while for $X \geq 0.67$ dL/L abruptly increases at the anomaly. Because our samples are polycrystals, the meaning of dL/L is not really clear but it is reasonable to conclude that the features of the lattice deformation at the anomaly are different for $X \leq 0.60$ and $X \geq 0.67$. Detailed features of the lattice distortion at the anomalies must be clarified by diffraction studies. For $X = 0.90$, the anomaly of dL/L is not discernible above 100 K. Preliminary results of dL/L for the $La_{0.33}Ca_{0.67}MnO_3$ polycrystals show the same behavior as that of $La_{0.33}Ca_{0.67}MnO_3$.[21]

Based on the various anomalies observed, let us dis-

LETTERS
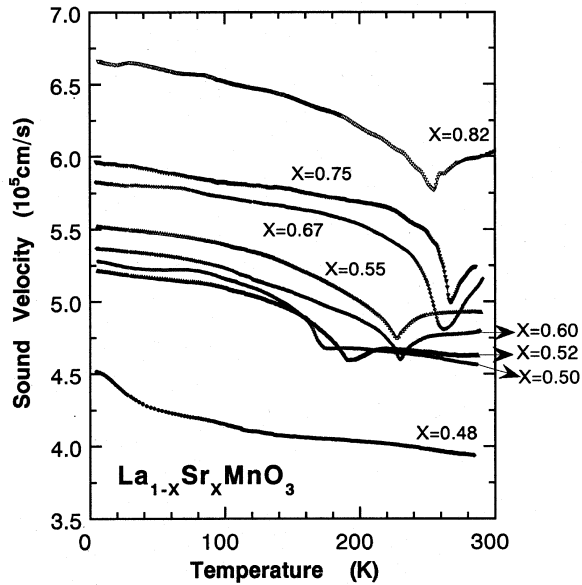

Fig. 3. Sound velocity $v_s(T)$ vs T for typical $La_{1-X}Sr_XMnO_3$ samples. Large anomalies associated with the charge-ordering transition are clearly seen. Note that $v_s(T)$ anomalously increases at around 50 K for $La_{0.52}Sr_{0.48}MnO_3$ in which the charge-order transition is not confirmed by other measurements.

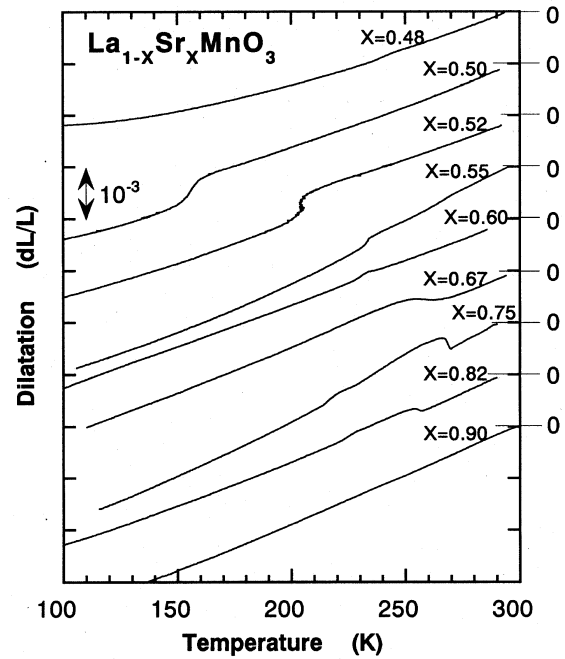Fig. 4. The dilatation $dL(T)/L$ of $La_{1-X}Sr_XMnO_3$ samples as a function of temperature T. Sudden changes of $dL(T)/L$ can be seen except for $X = 0.48$ and $X = 0.90$. The behavior at the anomaly changes its character between $X = 0.60$ and $X = 0.67$.

cuss the overall phase diagram of $La_{1-X}Sr_XMnO_3$ as a function of T and X. The charge-ordering phase transitions similar to those of present $La_{1-X}Sr_XMnO_3$ have been confirmed for several compounds, and the $M(T)$ curves given in Fig. 1 are quite similar to those of $La_{1-X}Ca_XMnO_3$.[4] For $La_{1-X}Ca_XMnO_3$ with $X \approx 2/3$, Ramirez et al.[22] observed the CO transition with a modulation wavelength $\boldsymbol{q} = (2\pi/a)(1/3, 0, 0)$. For similar samples, they also observed $v_s(T)$ anomalies just like the ones we have observed for $La_{1-X}Sr_XMnO_3$ in this study. Thus it seems almost indubitable that the anomalies in $v_s(T)$ and the dilatation dL/L are also due to the CO transitions in $La_{1-X}Sr_XMnO_3$ and the presented data suggest that the CO transitions occur for $0.48 \leq X \leq 0.82$ over a wide region of the Sr concentration.

On the basis of the data obtained in this work and in the previous reports,[19,20] we have constructed an overall phase diagram with particular emphasis on the charge-ordering transitions. The proposed phase diagram is shown in Fig. 5. The Sr composition X is plotted in the nominal quantity. Except for in the vicinities of $X = 0$ and $X = 1$, the phase diagram is fundamentally composed of three types of charge transitions, central compositions of which are located at $X = 1/8$ (CO-I), $1/2$ (CO-II) and (tentatively) $2/3$ (CO-III). Since the anomaly of the dilatation changes its feature between $X = 0.60$ and $X = 0.67$ and the absolute values of $\rho(T)$ jump there as well, we postulate that the character of the CO transitions also changes at around $X \approx 0.62$. Because dL/L of $La_{0.33}Ca_{0.67}MnO_3$ shows a similar increase to that of $La_{0.33}Sr_{0.67}MnO_3$ with decreasing temperature,[21] we infer that the modulation wavelength of CO-III of $La_{1-X}Sr_XMnO_3$ is also $\boldsymbol{q} = (2\pi/a)(1/3, 0, 0)$, intrinsically the same value as $La_{0.33}Ca_{0.67}MnO_3$.[22] In
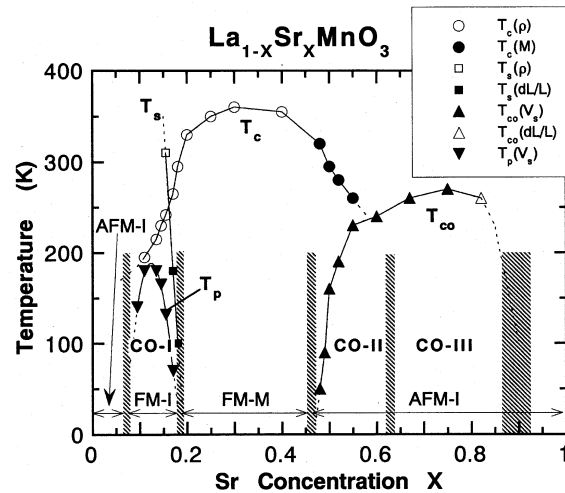

Fig. 5. The proposed phase diagram of $La_{1-X}Sr_XMnO_3$ system based on the present work and the data from ref. 19 ($X \leq 0.175$). T_c shows the Curie temperature which is determined from the $\rho(T)$ [O] and $M(T)$ [●] values. T_s shows the structural transition temperature which is determined from the $\rho(T)$ [□] and the dilatation $dL(T)/L$ [■] values. T_{co} shows the charge-ordering temperature determined from the $v_s(T)$ [▲] and the $dL(T)/L$ [△] values. T_p shows the polaron-ordering temperature determined from the $v_s(T)$ minimums[19] [▼]. The data point for $X = 0.09$ which is not contained in ref. 19 is added to this figure. The shaded regions correspond to the borders of the three types of charge orderings (CO-I, CO-II and CO-III). AFM-I, FM-I and FM-M imply antiferromagnetic insulator, ferromagnetic insulator and ferromagnetic metal, respectively.

Figs. 3 and 4, however, the anomalies in $v_s(T)$ and dL/L are almost the same in magnitude for $X = 0.67$ and 0.75 and we cannot exactly determine whether CO-III is cen-

tered at $X = 2/3$ or $X = 3/4$ from only the experimental observations performed in this study.

As we have already mentioned, Akimoto *et al.*[18] found the A-type AFM order for $La_{0.46}Sr_{0.54}MnO_3$ and confirmed that the A-type order is a very stable and fundamental magnetic structure at around $X = 0.54$. The A-type AFM order consists of alternative ferromagnetically ordered layers. On the other hand, Wollman and Koehler[3] observed the C-type AFM order for $La_{0.2}Ca_{0.8}MnO_3$ and Jirak *et al.*[23] also observed the C-type order for $Pr_{0.2}Ca_{0.8}MnO_3$. The C-type order, which consists of ferromagnetic chains, seems to be stabilized in a large X region. It may be possible that the AFM structures of the present $La_{1-X}Sr_XMnO_3$ crystals also change from the A-type in the CO-II region to the C-type in the CO-III region. As we have noticed in Fig. 2, the magnitude of the electrical resistivity shows an abrupt increase between $X = 0.60$ and $X = 0.67$. The relatively smaller $\rho(T)$ for $0.5 \leq X \leq 0.6$ is consistent with the A-type AFM order, because the ferromagnetic layers in the A-type structure are expected to contribute to the electrical conduction more effectively than the ferromagnetic linear chains in the C-type structure as a remnant of the double exchange interaction in this system.[18] It would be interesting and highly desirable to confirm whether the CE-type AFM structure, which is usually stable in a narrow region around $X = 0.50$, is realized or not in this system. The phase diagram in Fig. 5 is based only on the anomalies observed in the temperature dependences of $\rho(T)$, $M(T)$, $v_s(T)$ and $dL(T)/L$. A more detailed and exact diagram is expected to contain minute structural transformation lines such as the $O^* \to O' \to O^*$ reentrant transition observed by Kawano *et al.*[24] In order to complete the phase diagram given in Fig. 5, it is absolutely necessary to perform detailed neutron diffraction and/or electron diffraction studies.

In summary, we have measured the electrical resistivity $\rho(T)$, the magnetization $M(T)$, the sound velocity $v_s(T)$ and the dilatation $dL(T)/L$ of $La_{1-X}Sr_XMnO_3$ as a function of temperature T and have observed anomalies which are associated with the charge-ordering transitions. Based on the anomalies, we proposed a phase diagram of the $La_{1-X}Sr_XMnO_3$ system from the viewpoint of the charge ordering. The framework of the phase diagram is based upon three kinds of charge orderings centered at $X = 1/8, 1/2$ and $2/3$ (or $3/4$). In the regions of X where the charge ordering occurs, the system is nonmetallic at low temperatures. The metallic behavior of $\rho(T)$ persists to low temperatures only in the X region where the charge ordering is absent ($0.18 \leq X \leq 0.45$). The overall phase diagram of $La_{1-X}Sr_XMnO_3$ appears to be quite similar to that of $La_{1-X}Ca_XMnO_3$ in spite of the differences in the e_g-electron bandwidth.

1) A. Urushibara, Y. Moritomo, T. Arima, A. Asamitsu, G. Kido and Y. Tokura: Phys. Rev. B **51** (1995) 14103.
2) G. H. Jonker and J. H. van Santen: Physica (Utrecht) **16** (1950) 337.
3) E. O. Wollman and W. C. Koehler: Phys. Rev. **100** (1955) 545.
4) P. Schiffer, A. P. Ramirez, W. Bao and S.-W. Cheong: Phys. Rev. Lett. **75** (1995) 3336.
5) P. G. Radaelli, D. E. Cox, M. Marezio, S.-W. Cheong, P. E. Schiffer and A. P. Ramirez: Phys. Rev. Lett. **75** (1995) 4488.
6) A. J. Millis, P. B. Littlewood and B. I. Shraiman: Phys. Rev. Lett. **74** (1995) 5144.
7) A. J. Millis, B. I. Shraiman and R. Mueller: Phys. Rev. Lett. **77** (1996) 175.
8) Y. Yamada, O. Hino, S. Nohdo, R. Kanao, T. Inami and S. Katano: Phys. Rev. Lett. **77** (1996) 904.
9) Z. Jirak, S. Krupicka, Z. Simsa, M. Dlouha and Z. Vratislav: J. Magn. Magn. Mater. **53** (1985) 153.
10) E. Pollert, S. Krupicka and E. Kuzumicova: J. Phys. Chem. Solids **43** (1982) 1137.
11) Y. Tomioka, A. Asamitsu, Y. Moritomo and Y. Tokura: Phys. Rev. B **53** (1996) R1689.
12) H. Yoshizawa, H. Kawano, Y. Tomioka and Y. Tokura: J. Phys. Soc. Jpn. **65** (1996) 1043.
13) K. Knizek, Z. Jirak, E. Pollet, F. Zounova and S. Vratislav: J. Solid State Chem. **100** (1992) 292.
14) Y. Tomioka, A. Asamitsu, Y. Moritomo, H. Kuwahara and Y. Tokura: Phys. Rev. Lett. **74** (1995) 5108.
15) H. Kawano, R. Kajimoto, H. Yoshizawa, Y. Tomioka, H. Kuwahara and Y. Tokura: Phys. Rev. Lett. **78** (1997) 4253.
16) H. Kuwahara, Y. Tomioka, A. Asamitsu, Y. Moritomo and Y. Tokura: Science **270** (1995) 961.
17) H. Kawano, R. Kajimoto, M. Kubota and H. Yoshizawa: Phys. Rev. B **53** (1996) 2202.
18) T. Akimoto, Y. Maruyama, Y. Moritomo, A. Nakamura, K. Hirota, K. Ohoyama and M. Ohashi: Phys. Rev. B **57** (1998) 1.
19) H. Fujishiro, M. Ikebe, K. Konno and T. Fukase: J. Phys. Soc. Jpn. **66** (1997) 3703.
20) H. Fujishiro, M. Ikebe and K. Konno: J. Phys. Soc. Jpn. **67** (1998) 1799.
21) H. Fujishiro, T. Kikuchi and M. Ikebe: unpublished.
22) A. P. Ramirez, P. Schiffer, S.-W. Cheong, C. H. Chen, W. Bao, T. T. M. Palstra, P. L. Gammel, D. J. Bishop and B. Zegarski: Phys. Rev. Lett. **76** (1996) 3188.
23) Z. Jirak, S. Krupicka, Z. Simsa, M. Dlouha and S. Vratislav: J. Magn. Magn. Mater. **53** (1985) 153.
24) H. Kawano, R. Kajimoto, M. Kubota and H. Yoshizawa: Phys. Rev. B **53** (1996) R14709.